

The use of a Radial Drift TPC
in the
Hall D Detector at Jefferson Lab

Curtis A. Meyer

February 29, 2000

1 Introduction

One possible tracking configuration that has been proposed for the HALL D detector at Jefferson Lab is a *Radial TPC*. In this document, I want to review the pros and cons of such a detector within the HALL D framework. A radial TPC is different from a conventional TPC in that the drift path is perpendicular to the magnetic field direction, rather than parallel to it as in a conventional TPC. The ionization electrons are drifted radially outward to the outer surface of the TPC where the charge is collected by position sensitive detectors. In the HALL D design, the chamber would have an inner radius of as little as a few centimeters, and extend outward to about 60 cm. The length of the chamber could in principle be as long as the magnet, and given that the chamber is a TPC, each measurement would be a full space-point.

Most of the information in this paper has been obtained from the STAR collaboration, and the CERES collaboration. Both groups are currently operating such chambers in heavy ion experiments. A series of two nice papers from the STAR group on the behavior of radial TPC can be found in references [1] and [2]. Reference [3] is a nice report on the performance of the CERES detector.

The CERES detector has a length of 2 m, and inner radius of 48.6 cm and an outer radius of 132 cm. It uses an atmospheric pressure, Ne(80%) CO₂(20%) gas mixture. The electric field varies between 0.2 kV/cm and 0.6 kV/cm, and has a drift velocity that varies from 0.7 cm/ μ s to 2.4 cm/ μ s. For primary ionization produced at a radius of 120 cm and drifting outward, a resolution of 330 μ m in the azimuthal direction and 770 μ m in the radial direction has been achieved.

The STAR group has studied several gas mixtures for use in their radial TPC. They have looked at Ar(90%) CH₄(10%), Ar(50%) DME(50%) and Ar(50%) CO₂(50%). The chamber will operate in a region where the magnetic field is about 0.5 T, and uniform to about 5%. The chamber has an inner radius of about 13 cm and an outer radius of about 42 cm.

1.1 A Radial TPC for hall d

Reference [2] contains a large amount of data on drift properties in the STAR radial TPC. I have copied some of the plots for an Ar(50%)-CO₂(50%) gas mixture into this report. Figure 1 shows the transverse diffusion coefficient as a function of the electric field strength, while figure 2 shows the Longitudinal diffusion coefficient. Both of these appear to be independent of the magnetic field strength, but require an electric field of at least 400 V/cm to saturate them. Figure 3 shows the drift velocity as a function of the electric field strength. This has the typical linear dependence on E as seen in slow gases, and appears fairly insensitive to the magnetic field strength. Figure 4

shows the Lorentz angle as a function of both the electric and magnetic field strengths. It is fairly independent of the electric field, but varies linearly with the magnetic field strength.

If we now assume a radial TPC whose inner radius is 10 cm and whose outer radius is 60 cm. The electric field in such a configuration is given as follows.

$$\vec{E}(r) = \frac{V_c}{\ln(r_{\text{out}}/r_{\text{in}})} \frac{-\hat{r}}{r} \quad (1)$$

If we want the minimum electric field strength to be about 200 V/cm, then we find we need a cathode voltage of about 22 kV. This would yield a maximum field strength of about 1200 V/cm at the inner radius. Extrapolating the drift velocities from figure 3, we find that it varies from about 1.7 cm/ μ s at the inner radius to about 0.3 cm/ μ s at the outer radius. We can also extrapolate that the Lorentz angle from figure 4 will be about 18° at a 2.25 T field strength. Both of these effects will make the time-to-position relationship complicated, but not impossible to deal with.

The more significant effect in the radial TPC will be the diffusion of the drifting electron cloud. In a normal TPC, there is a natural focusing that occurs, and prevents the electrons from spreading in either the radial or the azimuthal directions. Because of this, a typical chamber can achieve on the order of 200 μ m resolution in these measurements. The diffusion along the length of the drift path then produces a smearing in z that gets worse with longer drift lengths. For two meters of drift, z resolutions on the order of 1 to 2 mm are not uncommon.

In a radial chamber, we do not have the trapping of electrons around magnetic field lines, and as such we need to worry about diffusion in all dimensions. The electron cluster width will evolve according to equation 2 in the radial direction:

$$\sigma_r^2(r + dr) = D_L^2(r) \cdot dr + \sigma_r^2(r) \cdot \left[1 + \frac{\partial v}{\partial r} \frac{dr}{v(r)} \right]^2 \quad (2)$$

If we assume that $\frac{\partial v}{\partial r} = 0$ and that D_L is a constant, then we can integrate equation 2 to yield:

$$\sigma_r^2 \approx D_L^2(r_{\text{final}} - r_{\text{initial}}). \quad (3)$$

Similarly, the azimuthal width evolves as in equation 4.

$$\sigma_{r\phi}^2(r + dr) = D_T^2(r) \cdot dr + \sigma_{r\phi}^2(r) \cdot \left[1 + \frac{dr}{r} \right]^2 \quad (4)$$

In the case of D_T being constant, and to first order in dr , we can integrate equation 4 to yield equation 5.

$$\sigma_{r\phi}^2(r) \approx D_T^2 \left[(r_{\text{final}} - r_{\text{initial}}) \frac{r_{\text{final}}}{r_{\text{initial}}} \right] \quad (5)$$

In the case where D_L and D_T are the same, equation 5 reduces down to:

$$\sigma_{r\phi}^2(r) = \sigma_r^2(r) \frac{r_{\text{final}}}{r_{\text{initial}}} \quad (6)$$

There is one last point to observe. The azimuthal resolution is measured at the collection surface, r_{final} , but in fact this needs to be traced back into the point where the hit was produced.

$$\sigma_{r\phi}(r_{\text{initial}}) = \sigma_{r\phi}(r_{\text{final}}) \frac{r_{\text{initial}}}{r_{\text{final}}} \quad (7)$$

Using the approximate forms, I have plotted the estimated radial, azimuthal and $r\phi$, (projected back to the initial radius) resolution as a function of the starting radius in figure 5. The numbers estimated here are not far off from the values quoted for the CERES detector [3].

The resolution is worst for tracks which are at small initial radius, and improves as the track radius approaches the outer cylinder wall of the chamber. With appropriate pad structure for readout, it may be possible to improve the azimuthal resolution, but the radial term is essentially limited to what is shown in the figure. In order for all resolutions to be better than $200 \mu\text{m}$, it is necessary for the primary track to have started at about $r = 55 \text{ cm}$. What is particularly bad is that many of the high momentum tracks never get outside a radius of about 25 cm . For these tracks where very good resolution is needed, the chamber is doing a very poor job.

2 Summary and Conclusions

Based solely on resolution issues, a radial TPC seems unlikely to be able to replace the forward packages of planar drift chambers. Monte Carlo studies indicate a significant improvement in detector resolution if the $r\text{-}\phi$ resolution of those chambers is decreased from $200 \mu\text{m}$ to $100 \mu\text{m}$. (This can be seen in Fig. 6) In addition, as these are fixed wire planes, the z resolution is anticipated to be extremely good. Of course a more detailed simulation is necessary to check the exact effect, but it seems that we will not be able to fill the entire tracking volume with one chamber.

However, the possibility of replacing the straw-tube chamber with a radial drift TPC cannot be excluded at this point. Additional work is necessary to understand the effect of such a chamber.

References

- [1] F. Paul Brady and Juan L. Romero, *Expressions for Diffusion in Radial Drift TPC's*, **STAR Note 64**.

- [2] X. Bittl, *et al.* *Diffusion and Drift Studies of Ar-DME/CO₂/CH₄ gas mixtures for a radial TPC in the $\mathbf{E} \perp \mathbf{B}$ field*, (1997).
- [3] A. Marín *et al.*, (The CERES Collaboration), *First results from the CERES radial TPC*.

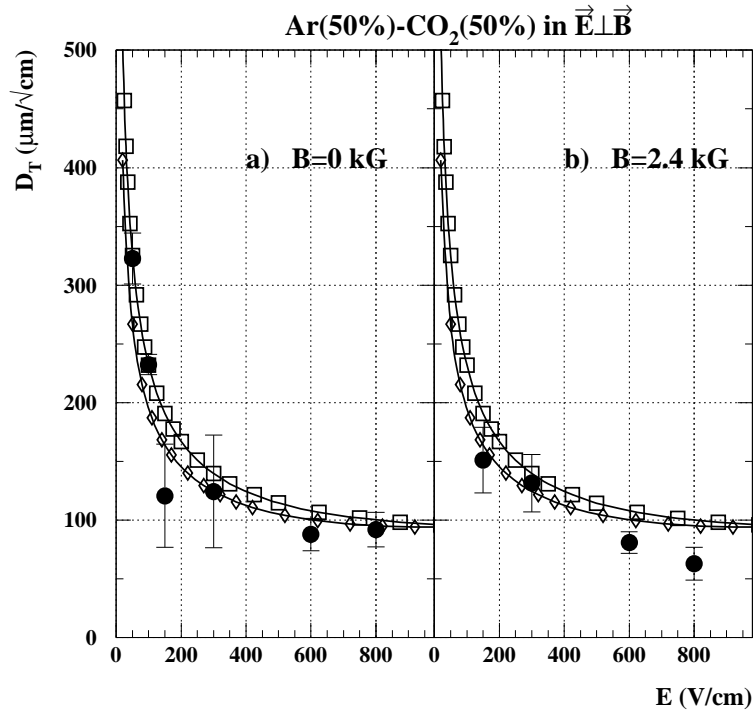


Figure 1: Transverse diffusion coefficient of Ar(50%)-C₂(50%) gas mixture as a function of the drift field for: (a) $B = 0kG$; (b) $B = 2.4kG$. The plots show data points (\bullet), calculations using the moments method (\square), and calculations using the Magbolts program (\diamond); smooth curves were drawn to connect the results of the calculations. (Figure taken from reference [2].)

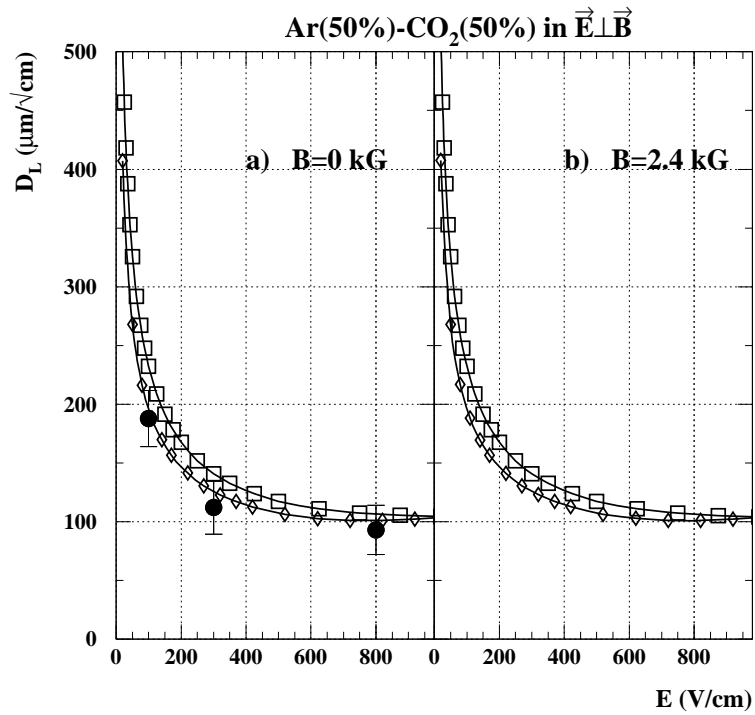


Figure 2: Longitudinal diffusion coefficient of Ar(50%)-C₂(50%) gas mixture as a function of the drift field for: (a) $B = 0$ kG; (b) $B = 2.4$ kG. The plots show data points (●), calculations using the moments method (□), and calculations using the Magbolts program (◇); smooth curves were drawn to connect the results of the calculations. (Figure taken from reference [2].)

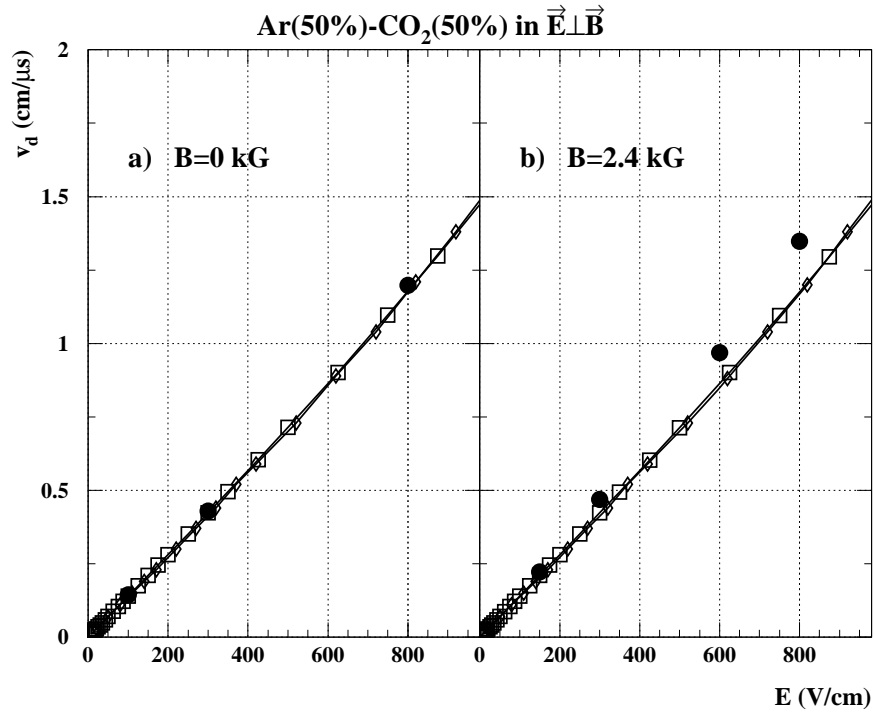


Figure 3: Drift velocities of the Ar(50%)-CO₂(50%) gas mixture as a function of the drift field for: (a) $B = 0$ kG; (b) $B = 2.4$ kG. The plots show data points (●), calculations using the moments method (□), and calculations using the Magbolts program (◇); smooth curves were drawn to connect the results of the calculations. (Figure taken from reference [2].)

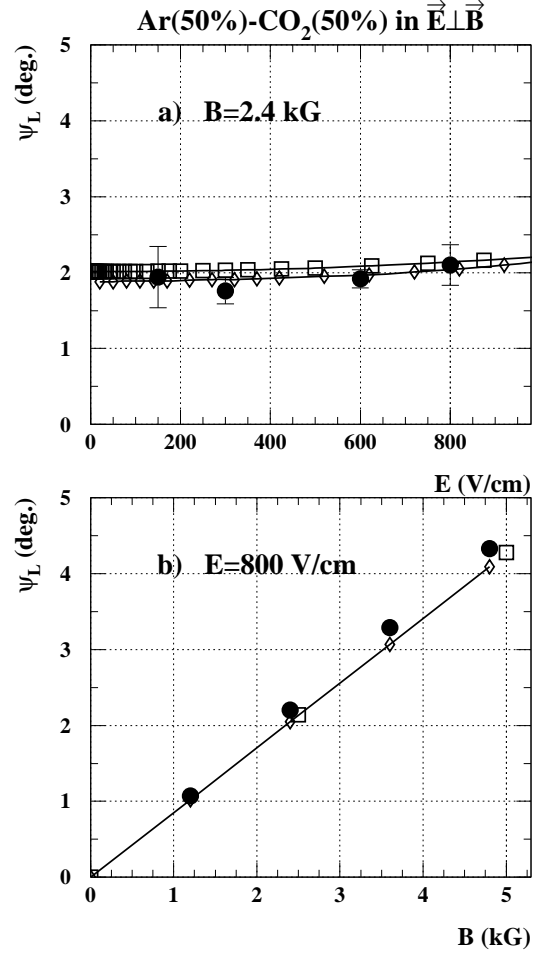


Figure 4: Lorentz angles of Ar(50%)-CO₂(50%) gas mixture as a function of the drift field for: (a) $B = 0$ kG; (b) $B = 2.4$ kG. The plots show data points (\bullet), calculations using the moments method (\square), and calculations using the Magbolts program (\diamond); smooth curves were drawn to connect the results of the calculations. (Figure taken from reference [2].)

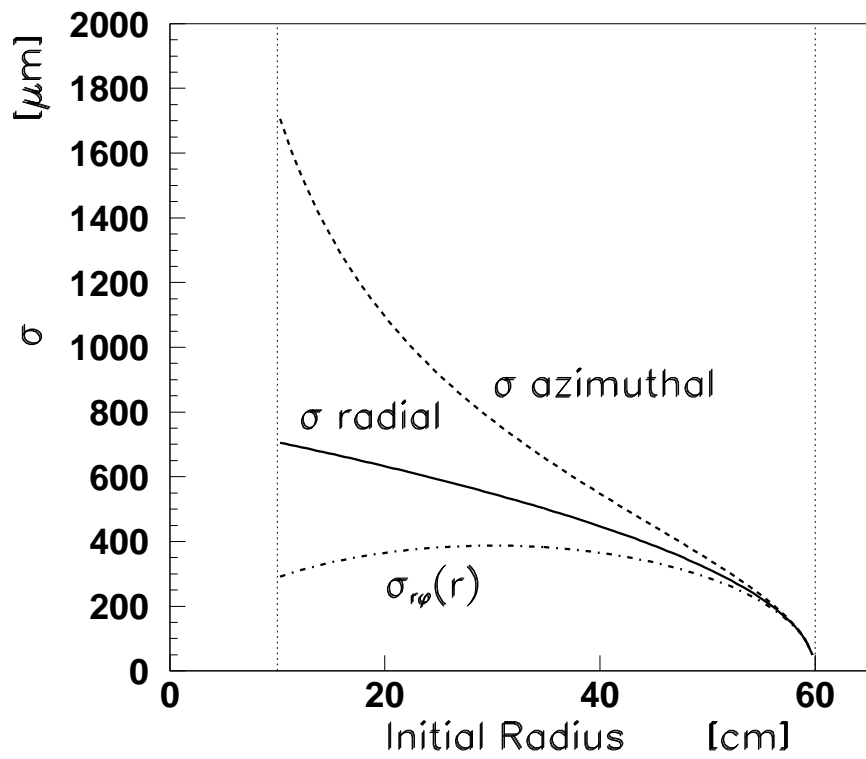


Figure 5: Estimated radial and azimuthal resolution in a HALL D radial drift TPC as a function of the radius of the hit.

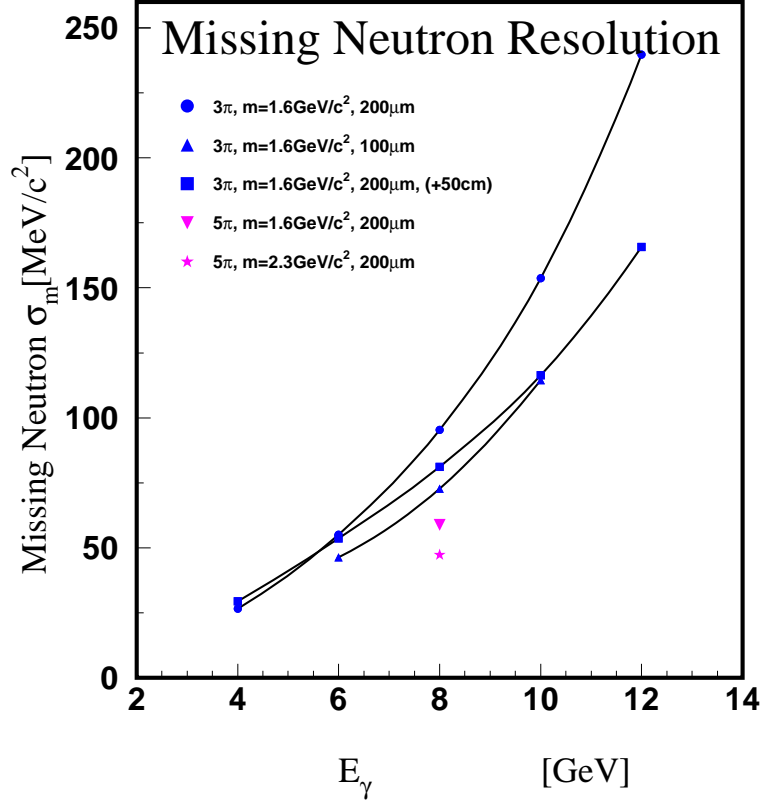


Figure 6: Missing neutron resolution from the reaction $\gamma p \rightarrow (3\pi)(5\pi)n$ as a function of photon beam energy. The various curves correspond to different assumptions in tracking reconstruction. ● is for a $1.6 \text{ GeV}/c^2$ 3π system with $200 \mu\text{m}$ resolution in the forward chambers. △ is the same as ●, except the resolution in the forward chambers is $100 \mu\text{m}$. □ is the same as ●, except we have added an additional coil to the magnet. ▽ is the same as ●, except we have a 5π system, and ★ is the same as ▽, except the 5π system has a mass of $2.3 \text{ GeV}/c^2$.